Remote Sensing Monitoring of Tobacco Field Based on Phenological Characteristics and Time Series Image —A Case Study of Chengjiang County, Yunnan Province, China

PENG Guangxiong[1], DENG Lei[2], CUI Weihong[1], MING Tao[3], SHEN Wei[4]

(*1. Institute of Remote Sensing Applications, Chinese Academy of Sciences, Beijing 100101, China; 2. College of Resource Environment and Tourism, Capital Normal University, Beijing 100048, China; 3. Institute of Geographic Sciences and Natural Resources Research, Chinese Academy of Sciences, Beijing 100101, China; 4. The Key Laboratory of Shanghai Education Commission for Oceanic Fisheries Resources Exploitation, College of Marine Sciences, Shanghai Ocean University, Shanghai 201306, China*)

Abstract: Using three-phase remote sensing images of China-Brazil Earth Resources Satellite 02B (CBERS02B) and Landsat-5 TM, tobacco field was extracted by the analysis of time series image based on the different phenological characteristics between tobacco and other crops. The spectral characteristics of tobacco and corn in luxuriant growth stage are very similar, which makes them difficult to be distinguished using a single-phase remote sensing image. Field film after tobacco seedlings transplanting can be used as significant sign to identify tobacco. Remote sensing interpretation map based on the fusion image of TM and CBERS02B's High-Resolution (HR) camera image was used as standard reference material to evaluate the classification accuracy of Spectral Angle Mapper (SAM) and Maximum Likelihood Classifier (MLC) for time series image based on full samples test method. SAM has higher classification accuracy and stability than MLC in dealing with time series image. The accuracy and Kappa of tobacco coverage extracted by SAM are 83.4% and 0.692 respectively, which can achieve the accuracy required by tobacco coverage measurement in a large area.

Keywords: tobacco; phenological characteristics; time series image; remote sensing

1 Introduction

The extraction of crop based on remote sensing has been widely used in regional agricultural management and agricultural research (MacDonald and Hall, 1980; Delecolle et al., 1992; Clevers and Van Leeuwen, 1996; David and Gregory, 2004; Zhang et al., 2008). Tobacco is a very important economic crop in China due to its high level of tax revenue. In view of the health hazards of tobacco, the Chinese Government attaches great importance to tobacco production. The planting area and distribution of tobacco is an important reference for tobacco production management, layout optimization and planting regulation. It is also of great significance to control the amount of tobacco production and safeguard the tobacco market. Remote sensing technology serves as a low-cost but highly efficient method capable of providing an important technical foundation for accurate extraction of crop planting area (Guerif and Duke, 2000; DeWit and Clevers, 2004; Doraiswamy et al., 2005; Xiao et al., 2005). Since the 1970s, the United States and other developed countries have established remote sensing measurements of crop planting area and crop yield estimation (Moran et al., 1997; Tso and Mather, 1999; Launay and Guerif, 2005). China has also carried out the research about the theories, methods and operations of the crop cultivation area measurement and yield estimation using remote sensing technology (Wu and Liu, 1997; Peng et al., 2006; Ma et al., 2008; Han et al., 2007; Li et al., 2008). Remote sensing researches on the

crops were mostly concentrated in wheat, rice, corn, and other major crops. Nevertheless, the researches on remote sensing monitoring of tobacco planting area were relatively less and need more in-depth researches and development (Claus et al., 1994; Narayanan et al., 1999; Ray and Dadhwal, 2001; Mei et al., 2006; Li et al., 2007). Remote sensing monitoring of tobacco planting area faces three major challenges: first, the spatial distribution of tobacco is very scattered; second, tobacco and other crops are often mixed planting; third, the spectral characteristics of tobacco and corn are very similar, so it is difficult to distinguish them using only leaf spectral characteristics. Therefore, it is very important to improve the universality of remote sensing monitoring method and extraction accuracy of tobacco planting area to promote the revolution from traditional agriculture to modern one in tobacco industry.

In this paper, three-phase satellite remote sensing images of a case study area were used to extract tobacco planting area based on the different phenological characteristics and time series spectral characteristics between tobacco and other crops.

2 Data and Methodology

2.1 Study area

The case study area is located in the eastern part of Chengjiang County, Yunnan Province, China (Fig. 1). The study area belongs to subtropical monsoon climate, with great changes in the terrain and distinct tridimensional climate. It has an average elevation of about 1528m, average annual temperature of 16.8℃, average annual precipitation of 960mm, frost-free period of 274d, and adequate sunlight and distinct temperature difference between day and night. It is a very typical tobacco planting region in Yunnan Province.
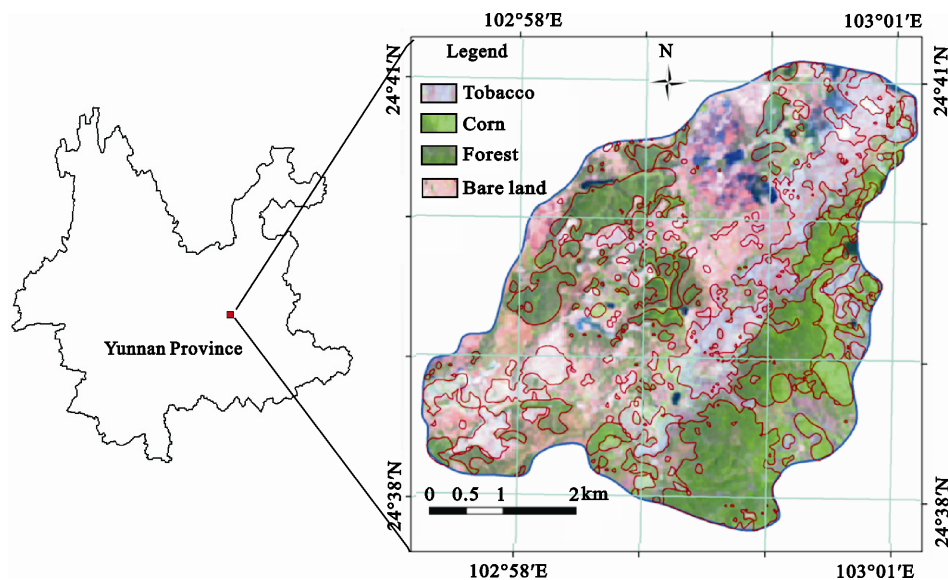

Fig. 1 TM image and location of study area

2.2 Data collection and preparation

The main remotely sensed data for this case study were from Charge Coupled Device (CCD) and High-Resolution (HR) camera of China-Brazil Earth Resources Satellite 02B (CBERS02B) and Landsat-5 TM images. The spatial resolutions for multi-spectral and panchromatic images of CBERS02B are 20m and 2.36m respectively. CCD bands 1–4 have similar band features with those of TM 1–4 bands. HR panchromatic image is suitable for visual interpretation based on the fusion with multi-spe-

ctral image. After comparing the quality of images and the phenological characteristics of tobacco and other crops, CCD and HR images on June 18, 2008, TM images on April 16 and May 24, 2008 were selected for this study.

TM and CCD are two different sensors with different performance and imaging conditions. Therefore radiation calibration and matching for two types of remote sensing images are very necessary. TM sensor has a stable and accurate radiation calibration coefficient and is suitable to be used as a reference image for the cross-ca-

libration of CCD sensor (Peng et al., 2007). Firstly, TM images are corrected based on the radiation calibration coefficient and resampled to the spatial resolution of 20m. Bare land and water were used as high and low reflectivity calibration subjects respectively. Secondly, choosing the same position point in the TM and CCD images to correct CCD using linear experience method with reference to TM. Finally, the radiation brightness of the same position point between CCD and TM were corrected to the same level.

CCD and TM images were georeferenced based on 1：50,000 scale topographical maps of the study area and the position errors were within one pixel. CCD bands 1–4 of one-phase and TM 1–5, 7 bands of two-phase were layer-stacked to a new 16-bands multi-spectral image with spatial resolution of 20m.

2.3 Spectrum analysis

2.3.1 Phenological characteristics
Corn is the crop most difficult to be distinguished from tobacco due to its similar spectral characteristics as to-bacco's. During its luxuriant growth stage of corn, TM spectrum of it is basically as same as that of tobacco and it is not the good time to distinguish corn and tobacco in remote sensing image. According to the different phenological characteristics of corn and tobacco, multi-temporal images can be used to distinguish them based on time series spectrum. In the study area, the sowing time of spring corn is from late March to early April and its mature time in the period from late August to early September. For spring corn, it needs to cover field film for seeds to raise the temperature. However, field film is not necessary for summer corn because sowing time from late May to early June is accompanying with high temperature. Finally, summer corn matures in the period from late October to early November. On the other hand, the transplanting time of tobacco is normally from late April to mid-May when field film is also needed to raise temperature. In early August, tobacco matures and begins entering the harvesting period. The phenological calendars of tobacco and corn of study area are indicated in Table 1.

Table 1 Phenological calendars of tobacco and corn in study area

Month	Mar.			Apr.			May			Jun.			Jul.			Aug.			Sep.			Oct.
Dekan-day	1	2	3	1	2	3	1	2	3	1	2	3	1	2	3	1	2	3	1	2	3	1	2	3
Tobacco	Seedlings nurture				Transplanting (film)		Rooting		Luxuriant growth			Maturing Harvesting										
Spring corn		Sowing (film)		Trefoil		Jointing			Heading			Maturing			Harvesting						
Summer corn							Sowing	Trefoil		Jointing		Heading			Maturing			Harvesting		

2.3.2 Analysis of field film spectrum
In late May, all tobacco seedlings have been transplanted to field and covered with the field film to improve accumulative temperature. There is a significant difference between field film of tobacco and other crops. Figure 2 shows the field picture and TM spectrum of tobacco field film. TM spectra of tobacco field film and bare land are similar but not identical. Because the mixed spectrum of tobacco field film composed by plastic film, tobacco seedlings and soil (Fig. 2a), tobacco field film has higher Normalized Difference Vegetation Index (NDVI) value than that of bare land and shows some vegetation spectral characteristic (Fig. 2b). Although it is difficult to distinguish tobacco and corn in luxuriant growt stage because of their similar spectrum, the spectrum of tobacco field film has significant difference with tobacco and corn in luxuriant growth stage, which is very useful to extract tobacco fields (Fig. 2b).

Corn field film appears in late March, while tobacco field film appears in mid-May. This provides a long time difference between them, which can eliminate the negative factor of their similar spectra. The time of summer corn sowing and tobacco transplanting are close, however tobacco will not be confused with summer corn because tobacco is covered with field film while summer corn is uncovered.

2.3.3 Analysis of time series spectrum
In the stacked 16 bands time series image, 12 groups' spectral curves of tobacco, spring corn and forest were collected. The average levels of 12 groups' spectral values were calculated and the average time series spectrum curves of tobacco, spring corn and forest were acquirable (Fig. 3). On April 16, the tobacco field was bare land for transplanting, while corn field was in the period of trefoil stage and retained some field film. In the TM image of April 16, tobacco field showed the

pure spectrum of bare land, while corn field showed the mixed spectrum of land, plastic film and corn (Fig. 3 and Fig. 4a). On May 24, tobacco has been transplanted for several days, while corn entered the late jointing with flourishing growth. In the TM image of May 24, tobacco field showed the mixed spectrum of land, plastic film and tobacco, while corn field mainly showed the spectral characteristics of vegetation with higher NDVI than tobacco field (Fig. 3 and Fig. 4b). On June 18, tobacco entered the luxuriant growth stage, while corn entered the heading stage. In the CCD image of June 18, tobacco and corn both show green with similar image characteristics and spectrum curves (Fig. 3 and Fig. 4c). From the above analysis we found that May 24 is the best phase to distinguish tobacco and corn when the field film is the most distinct sign to extract tobacco.
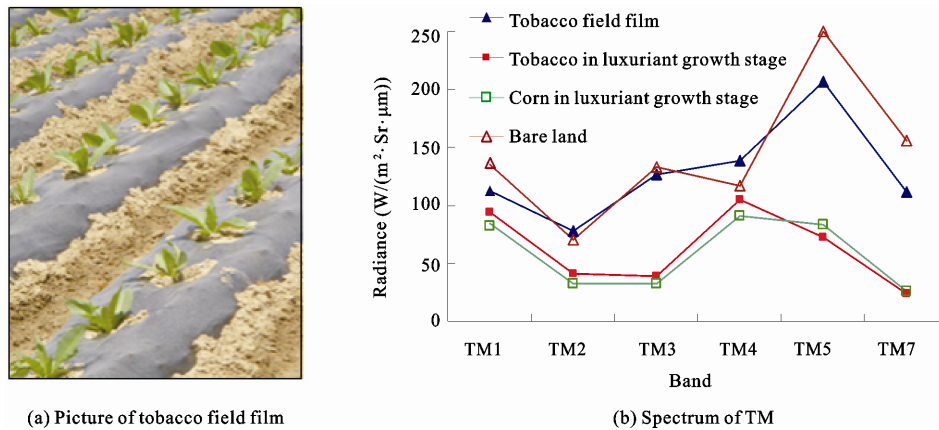

(a) Picture of tobacco field film   (b) Spectrum of TM

Fig. 2 Picture (a) and spectral characteristics (b) of tobacco field film
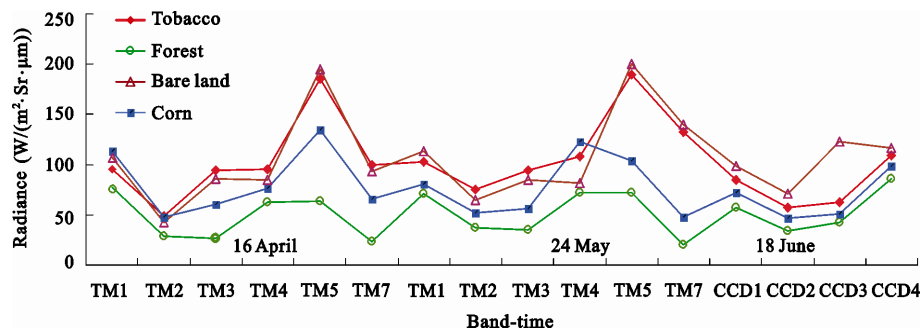
Fig. 3 Time series spectrum of typical land covers

(a) TM image of April 16   (b) TM image of May 24   (c) CCD image of June 18   (d) Classification map
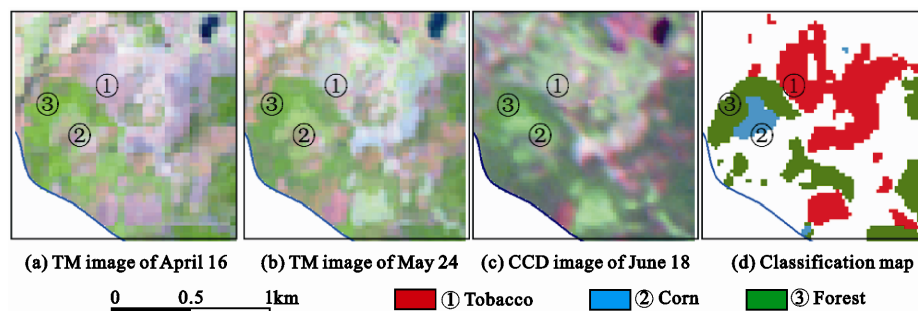
① Tobacco   ② Corn   ③ Forest

Fig. 4 Comparisons of vegetation feature in multi-temporal images

2.4 Extraction methods

Though conventional classification methods can be used to process time series images, it is difficult to make full use of time series advantages. Maximum Likelihood Classifier (MLC) is the most commonly and widely used classification method based on Bayes theory

(Conese and Maselli, 1992; Liang, 2001; Ming and Merrill, 2002). Since time series image and hyperspectral image both have high-dimensional characteristics, hyperspectral processing methods can also be used to proceess time series image. Spectral Angle Mapper (SAM) is a physically-based spectral classification that uses an *n*-dimensional angle to match pixels to reference spectra (Kruse et al., 1993). The algorithm determines the spectral similarity between two spectra by calculating the angle between the spectra, treating them as vectors in a space with dimensionality equal to the number of bands (Kruse et al., 1993). Though SAM is often used to deal with hyperspectral image, it is also found effective to deal with time series spectral (Xu et al., 2005). Visual interpretation is widely used in higher accuracy classification, especially in meter-scale high-resolution remote sensing images. In this paper, SAM, MLC and Visual interpretation was used to extract tobacco in order to compare the results of three different classification methods for time series images.

3 Results and Validation

3.1 Results

SAM and MLC supervised classifications were carried out in ENVI4.2 remote sensing process software. The average time series spectrum samples were used in SAM. Maximum Spectrum Angle Threshold (MSAT) of tobacco, corn and forest were identified as 0.11, 0.12 and 0.13 respectively. Classification results of SAM are shown in Fig. 5. Twelve training plots of tobacco, corn and forest were selected using ROI tool near the location where spectrum samples collected for MLC. The MLC operated with the Probability Threshold (PT) of 0.8. The area statistics of tobacco, corn and forest in the study area are shown in Table 2.

Since the spectral characteristics of tobacco field film in TM image of May 24 is prominent, this TM image was fused with HR panchromatic image of CBERS02B of June 18 based on Pansharp method in PCI software. The fused image with Pansharp method has good color fidelity and clear texture, which conduces to visual interpretation (Fig. 6a). The fused image and multi-temporal images were used for visual interpretation combined with GPS data collected in field. The areas of tobacco, corn and forest based on visual interpretation map are 421.3ha, 83.1ha and 594.1ha respectively

(Table 2). The visual interpretation map (Fig. 1, Fig. 6b and Fig. 6c), will be used as standard reference data to validate the classification of SAM and MLC.
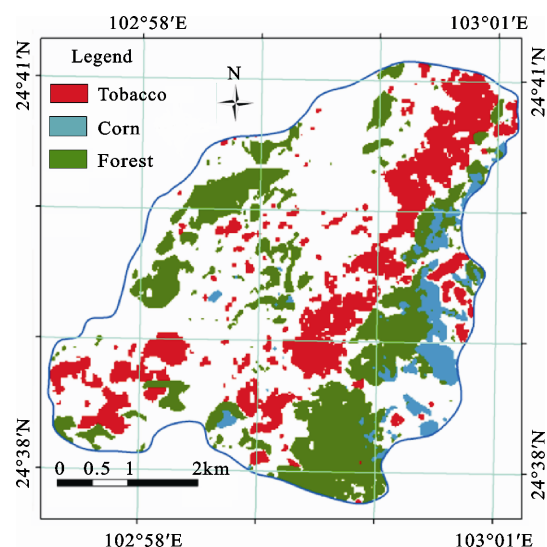

Fig. 5 Classification results of crops and forest based on SAM

Table 2 Crops and forest area acquisited by different classi-fiction methods (ha)

Class	MLC	SAM	VI
Tobacco	428.5	432.9	421.3
Corn	88.8	98.9	83.1
Forest	607.9	627.9	594.1

3.2 Validation

Conventional validation method of classification requires a certain number of randomly selected test pixels to be compared with actual category to calculate classification accuracy. However statistical sampling methods would have great influence on the assessment accuracy of classification (Congalton 1991; Stehman and Czaplewski, 1998; Liu et al., 2006). Full samples test method can avoid the uncertainty of statistical sampling and improve the accuracy of assessment results (Liu et al., 2006). Visual interpretation map based on field surveys has high classification accuracy and can be used as standard reference data for the assessment of automatic classification results. Vector data of visual interpretation were converted to raster data with a spatial resolution of 20m and keep the same category code with automatic classification results. Full samples test method was realized through superposition operation and code reclassification based on visual interpretation and automatic classification image (Han et al., 2007), the expression is
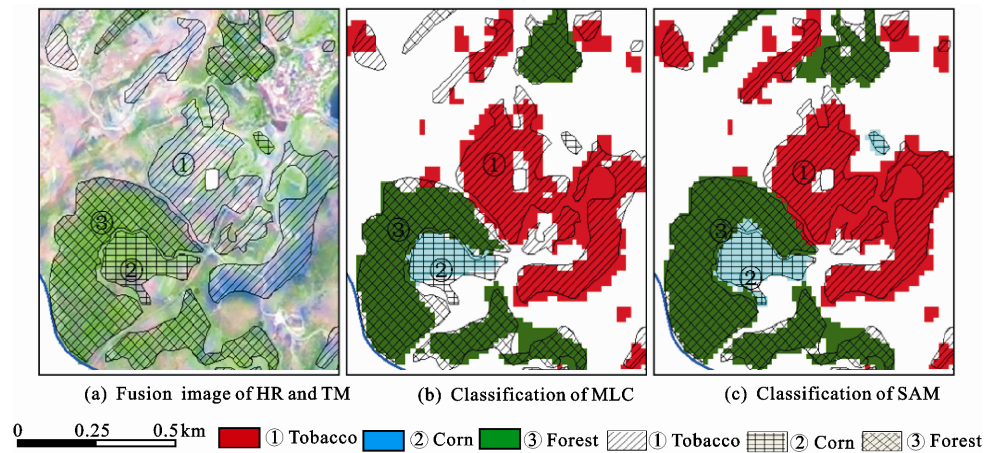
| (a) Fusion image of HR and TM | (b) Classification of MLC | (c) Classification of SAM |

0   0.25   0.5 km   ① Tobacco   ② Corn   ③ Forest   ① Tobacco   ② Corn   ③ Forest

Fig. 6 Classification results of crops and forest based on different methods

as follows.

$$C_{ij} = 10A_{ij} + B_{ij} \qquad (1)$$

where, C_{ij} is the pixel value of accuracy assessment image; A_{ij} is the pixel value of automatic classification image (SAM or MLC); B_{ij} is the pixel value of visual interpretation image.

The error matrix and classification accuracy of SAM and MLC can be calculated using full samples test method (Table 3). Table 3 shows that the overall Kappa of SAM and MLC are 0.713 and 0.690 while the overall accuracy of SAM and MLC are 84.9% and 82.2% respectively. Tobacco's overall Kappa and accuracy of SAM are 0.025 and 5.5% higher respectively than those of MLC, and this is coincident with the actual distribution of tobacco. Figure 6b and 6c are the classification results of MLC and SAM in a typical plot respectively. Generally speaking, SAM has higher capacity to extract tobacco and more advantages in dealing with time series remote sensing images than MLC. In MLC method, different operators may induce uncertainty/inconsistency of training samples and causes the differences of classification results. On the other hand, SAM obtains sample spectrum using the average values based on several groups' samples and it can greatly reduce the uncertainty of training samples caused by different operators. If the same Maximum Spectrum Angle Threshold (MSAT) is chosen, the classification results of SAM will have very high consistency. Therefore, SAM is more appropriate and effective than MLC to extract tobacco based on the time series remote sensing images.

Table 3 Error matrix of SAM and MLC classification

	Estimated image by SAM						Estimated image by MLC				
Class	Tobacco	Corn	Forest	Sum	Kappa	Class	Tobacco	Corn	Forest	Sum	Kappa
Tobacco	10812	523	1631	12966	0.692	Tobacco	10703	612	2413	13728	0.667
Corn	217	2471	300	2988	0.670	Corn	254	2217	327	2798	0.637
Forest	2263	221	15682	18166	0.737	Forest	2263	235	15182	17680	0.716
Sum	13292	3215	17613	34120	0.713	Sum	13220	3064	17922	34206	0.690
Accuracy of tobacco = 83.4%						Accuracy of tobacco = 77.9%					
Overall accuracy =84.9%						Overall accuracy =82.2%					

4 Conclusions and Discussion

The planting area and distribution of tobacco were extracted accurately using time series image based on the different phenological characteristics between tobacco and other vegetation, coupling with the special spectral peculiarity of tobacco field film. A few findings are summarized as below:

(1) It is difficult to extract tobacco in a single-phase remote sensing image due to its highly similar spectral characteristics with corn in the period of luxuriant growth. However time series image composed with multi-temporal images has demonstrated the capability to extract tobacco automatically by utilizing the different phenological characteristics between tobacco and other vegetation.

(2) SAM has higher classification accuracy and stability than MLC in dealing with time series remote sensing image.

(3) The key of tobacco extraction using time series remote sensing image is to acquaint the phenological characteristics of tobacco and other vegetation and to select the appropriate phases of remote sensing images that reflect the land cover features of various phenological periods.

(4) Rainy weather and cloud cover will have some adverse impact on acquiring high-quality time series remote sensing image. Multi-temporal high-resolution radar images will not be affected by weather condition and have high development potential. The feasibility of using time series radar image to extract tobacco will be studied in the following work.

Acknowledgments

References

Claus B, Eckehard N, Kalman S, 1994. Spectrometer for fast measurements of in vivo reflectance, absorptance, and fluorescence in the visible and near-infrared. *Remote Sensing of Environment*, 48(1): 18–24. DOI: 10.1016/0034-4257(94)90110-4.

Clevers J G P W, Van Leeuwen H J C, 1996. Combined use of optical and microwave remote sensing data for crop growth monitoring. *Remote Sensing of Environment*, 56(1): 42–51. DOI: 10.1016/0034-4257(95)00227-8.

Conese C, Maselli F, 1992. Use of error matrices to improve area estimates with maximum likelihood classification procedures. *Remote Sensing of Environment*, 40(2):113–124. DOI: 10.1016/0034-4257(92)90009-9.

Congalton R G, 1991. A review of assessing the accuracy of classifications of remotely sensed data. *Remote Sensing of Environmen*, 37(1): 35–46. DOI: 10.1016/0034-4257(91)90048-B.

David B L, Gregory P A, 2004. Cropland distribution from temporal unmixing of modis data. *Remote Sensing of Environment*, 93(3): 412–422. DOI: 10.1016/j.rse.2004.08.002.

Delecolle R, Maas S J, Guerif M et al., 1992. Remote sensing and crop production models: present trends. *ISPRS Journal of Photogrammetry & Remote Sensing*, 47(4): 145–161. DOI: 10.1016/0924-2716(92)90030-D.

DeWit A J W, Clevers J G P W, 2004. Efficiency and accuracy of perfield classification for operational crop mapping. *International Journal of Remote Sensing*, 25(1): 4091−4112. DOI:

10.1080/0143116031000161 9580.

Doraiswamy P C, Sinclair T R, Hollinger S et al., 2005. Application of MODIS derived parameters for regional crop yield assessment. *Remote Sensing of Environment*, 97(2): 192–202. DOI: 10.1016/j.rse.2005.03.015.

Guerif M, Duke C L, 2000. Adjustment procedure of a crop model to the site specific characteristics of soil and crop using remote sensing data assimilation. *Agriculture Ecosystems & Environment*, 81(1): 57–69. DOI: 10.1016/S0167-8809(00) 00168-7.

Han Lijian, Pan Yaozong, Jia Bin et al., 2007. Acquisition of paddy rice coverage based on multi-temporal IRS-P6 satellite AWiFS RS-data. *Transactions of the Chinese Society of Agricultural Engineering*, 23(5): 137–143. DOI: 1002-6819.0.2007-05-024. (in Chinese)

Kruse F A, Lefkoff A B, Boardman J B et al., 1993. The spectral image processing system (SIPS)-interactive visualization and analysis of imaging spectrometer data. *Remote Sensing of Environment*, 44(3): l45–l63. DOI: 10.1016/0034-4257(93)900-13-N.

Launay M, Guerif M, 2005. Assimilating remote sensing data into a crop model to improve predictive performance for spatial applications. *Agriculture Ecosystems & Environment*, 111(4): 321–339. DOI: 10.1016/j.agee.2005.06.005.

Li Hongjun, Zheng Li, Lei Yuping et al., 2008. Estimation of water consumption and crop water productivity of winter wheat in North China Plain using remote sensing technology. *Agricultural Water Management*, 95(11): 1271–1278. DOI: 10.1016/j.agwat.2008.05.003.

Li Xiangyang, Liu Guoshun, Yang Yongfeng et al., 2007. Relationship between hyperspectral parameters and physiological and biochemical indexes of flue-cured tobacco leaves. *Agricultural Sciences in China*, 6(6): 665–672. DOI: 10.1016/S16-71-2927(07)60098-4.

Liang S, 2001. Land-cover classification methods for multi-year AVHRR data. *International Journal of Remote Sensing*, 22(8): 1479–1493. DOI: 10.1080/01431160120833.

Liu Xulong, He Chunyang, Pan Yaozhong et al., 2006. Accuracy assessment of thematic classification based on point and cluster sample. *Journal of Remote Sensing*, 10(3): 366–373. DOI: 1007-4619.0.2006-03-012. (in Chinese)

Ma Yuping, Wang Shili, Zhang Li et al, 2008. Monitoring winter wheat growth in North China by combining a crop model and remote sensing data. *International Journal of Applied Earth Observation and Geoinformation*, 10(4): 426–437. DOI: 10.1016/j.jag.2007.09.002.

MacDonald R B, Hall F G, 1980. Global crop forecasting. *Science*, 208(4445): 670–679. DOI: 10.1126/science.208.4445.670

Mei Xin, Cui Weihong, Zhang Xuexia et al., 2006. Monitoring of tobacco planted acreage based on multiple remote sensing sources. In: *IEEE International Geoscience and Remote Sensing Symposium Proceedings*. Denver, USA: 668–670. DOI: 10.1109/IGARSS.2006.175.

Ming C H, Merrill K R, 2002. A subpixel classifier for urban land cover mapping based on a maximum-likelihood approach and

expert system rules. *Photogrammetric Engineering & Remote Sensing*, 68(11): 1173–1180.

Moran M S, Inoue Y, Barnes E M, 1997. Opportunities and limitations for image-based remote sensing in precision crop management.*Remote Sensing of Environment*, 61(3): 319–346. DOI: 10.1016/S0034-4257(97)00045-X.

Narayanan S, Oliver W, Hartmut K L, 1999. Changes in blue-green and chlorophyll fluorescence emission and fluorescence ratios during senescence of tobacco plants. *Remote Sensing of Environment*, 69(3): 215–223. DOI: 10.1016/S00344257(99)-00029-2.

Peng Guangxiong, He Yuhua, Li Jing et al., 2007. Study on CBERS2's CCD image cross calibration and atmospheric correction. *Journal of Infrared and Millimeter Waves*, 26(1): 22–27. DOI: 1001-9014.0.2007-01-004. (in Chinese)

Peng Guangxiong, Li Jing, Chen Yuhao et al., 2006. High-resolution surface relative humidity computation using MODIS image in peninsular Malaysia. *Chinese Geographical Science*, 16(3): 260–264. DOI: 10.1007/s11769-006-0260-6.

Ray S S, Dadhwal V K, 2001. Estimation of crop evapotranspiration of irrigation command area using remote sensing and GIS. *Agricultural Water Management*, 49(3): 239–249. DOI: 10.1016/S0378-3774(00)00147-5.

Stehman S V, Czaplewski R L, 1998. Design and analysis for thematic map accuracy assessment: Fundamental principles. *Remote Sensing of Environment*, 64(3): 331–334. DOI: 10.1016/S0034-4257(98)00010-8.

Tso B, Mather P M, 1999. Crop discrimination using multi-temporal SAR imagery. *International Journal of Remote Sensing*, (12): 2443–2460. DOI: 10.1080/014311699212119.

Wu Binfang, Liu Haiyan, 1997. The operational methods for rice area estimation using remote sensing. *Journal of Remote Sensing*, 1(1): 58–63. DOI: 1007-4619.0.1997-01-007. (in Chinese)

Xiao Xiangming, Boles S, Liu Jiyuan et al., 2005. Mapping paddy rice agriculture in southern China using multi-temporal MODIS images. *Remote Sensing of Environment*, 95(4): 480–492. DOI: 10.1016/j.rse.2004.12.009.

Xu Weidong, Yin Qiu, Kuang Dingbo, 2005. Comparison of different spectral match models. *Journal Infrared Millimeter and Waves*, 24(4): 296–231. DOI: 1001-9014.0.2005-04-012. (in Chinese)

Zhang Mingwei, Zhou Qingbo, Chen Zhongxin et al., 2008. Crop discrimination in Northern China with double cropping systems using fourier analysis of time-series MODIS data. *International Journal of Applied Earth Observation and Geoinformation*, 10(4): 476–485. DOI: 10.1016/j.jag.2007.11.002.